Heliyon 9 (2023) e16129

Contents lists available at ScienceDirect

Heliyon

journal homepage: www.cell.com/heliyon

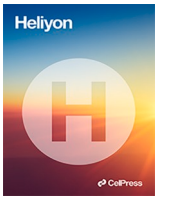

Research article

Theoretical study of effect of the geometrical parameters on the dynamic properties of the elastic rings of an air journal bearing

Ahmed M. Paridie *, Nicoleta M. Ene

University of Toledo, college of engineering, MIME department, USA

ARTICLE INFO

Keywords:
Vibration analysis
Artificial intelligence

ABSTRACT

The paper investigates theoretically the effect of the geometry of the elastic rings of an air journal bearing on the elastic rings dynamic coefficients. The physical finite element method (FEM) model used to obtain the dynamic coefficients of the rings is discussed. A theoretical model is implemented to predict the effect of the geometrical parameters on the dynamic coefficients of the elastic rings. The effect of the geometrical parameters on the dynamic coefficients at different frequencies is studied using FEM. The elastic geometry that result in desired dynamic coefficients is demonstrated. Since predicting the dynamic coefficients for all possible ring geometries using FEM would be computationally expensive. A neural network (NN) is trained to predict the dynamic coefficients for all possible ring geometries generated by the different ring geometrical parameters within a given input domain. The NN results are compared to the experimentally verified FEM results and the results are in good agreement.

1. Introduction

1.1. Literature review

Elastic rings are used to reduce vibrations and improve stability of systems. For example, they can be used to support the sleeve of air journal bearings. On one the major disadvantages of air bearings are the self-excited whirl that can appear at high rotational speeds. It makes them unstable and limits their range of applications. Introducing an elastic ring between the air bearing sleeve and housing it is possible to reduce the size of the regions of self-excited vibrations, or to eliminate them completely [1].

[2] proved theoretically that the elastic rings can increase the threshold velocity at which an oil or gas journal bearing becomes unstable. [70] verified experimentally that using O rings as elastic supports for pressurized air bearings results in minimizing the rotor whirl at high speeds. By adding O rings, they were able to increase the operating speed from 30,000 rpm to 110,000 rpm [3]. developed a mathematical model to calculate the onset whirl speed of an externally pressurized gas journal bearing supported on rubber 'O' rings. He concluded that stability of the bearing increases (onset whirl speed increases) when the O ring stiffness is increased [4]. studied theoretically and experimentally the effect of adding O rings on the static characteristics of an aerostatic journal bearing. He concluded that the load capacity of the bearing increases with decreasing the stiffness of the O-ring. The elastic rings can also be used in squeeze film dampers. Squeeze film dampers (SFD) are oil lubricated elements that provide damping to systems. They are widely used in aeroengine rotors to suppress high-level vibrations and improve the stability of the rotor-bearing systems. The stiffness and damping

* Corresponding author.
E-mail address: ahmed.paridie@rockets.utoledo.edu (A.M. Paridie).

https://doi.org/10.1016/j.heliyon.2023.e16129
Received 18 December 2022; Received in revised form 24 April 2023; Accepted 7 May 2023
Available online 22 May 2023

coefficients of conventional SFDs are highly non-linear, which results in bi-stable and non-synchronous responses of the rotors. The non-linear effects can be reduced if the oil film of the SFD is divided in two layers by embedding an elastic ring in the oil film [5]. proved theoretically that the stiffness of a squeeze film damper becomes linear when an elastic ring is added to the system [6]. constructed a test rig to verify experimentally the theoretical work of [5]. They concluded that the elastic ring stiffness and damping properties are approximately linear for small forces. They also calculated using the finite element method the steady state response of the rotor system for different elastic rings geometries. They concluded that when elastic rings are added to the SFD system, the resultant system has linear dynamic coefficients if the rotor eccentricity ratio is less than 0.7. The elastic rings can also be used to model different engineering structures. For example [7], modeled a disk-type winding of a power transformer by a stack of concentric rings coupled by elastic elements. First, they investigated analytically and experimentally the vibration characteristics of single circular rings and of single layers of axially and radially coupled rings. Then, they used the rings as building blocks for a stack of concentric rings connected by elastic insulators. The objective of this paper is to continue the work done by Ref. [8]) who designed an FEM model to theoretically study the dynamic properties of the elastic rings of an air dynamic journal bearing and designed a test rig to validate experimentally the theoretical results, the effect of the geometrical parameters on the dynamic coefficients of the elastic rings [8]) are studied in this paper to facilitate for designers the selection process of the ring geometry that would result in the desired dynamic coefficients for a designers prospective application. Since the ring geometrical parameters are continuous variables and obtaining the rings dynamic coefficients for all possible geometry combinations is computationally expensive, NNs are used to reduce the computational power of FEM simulations [8]) (see Fig. 1).

2. The development of an FEM model

The FEM model and lumped vibration model discussed in Ref. [8]) are used to obtain the FEM results dynamic coefficients for different elastic ring geometries. To demonstrate the FEM framework done by Ref. [8]), the elastic ring geometrical model shown in Fig. 2 and used by FEM model consists of a circular beam supported by inner and outer pads. The geometrical parameters which affect the dynamic characteristics of the elastic ring are the thickness and height of the beam, and the sector angle and number of the inner and outer pads [8]). The material type of the elastic geometry is proprietary hence not discussed in the paper.

2.1. Elastic rings constraints

In the air journal bearing setup, the ring is mounted between the bearing sleeve and housing as shown in Fig. 3 (a). This constrains the rings motion only to rotation about or translation along the longitudinal axis of the sleeve. During the shaft rotation, the moving sleeve applies dynamic loads on the ring inner pads, while the fixed housing supports the ring outer pads. To simplify the simulation model [8]), the loading and support positions are interchanged as shown in Fig. 4. In the simulations, the vibrating housing excites the ring outer pads, and a fixed pin supports the ring inner pads as shown in Fig. 3 (b).

The pads of the ring are interchanged to compensate for the interchanged constraints of the rings. For example, the outer pads supported by the journal bearing housing become the inner pads for the experimental and theoretical study. Similarly, the inner pads

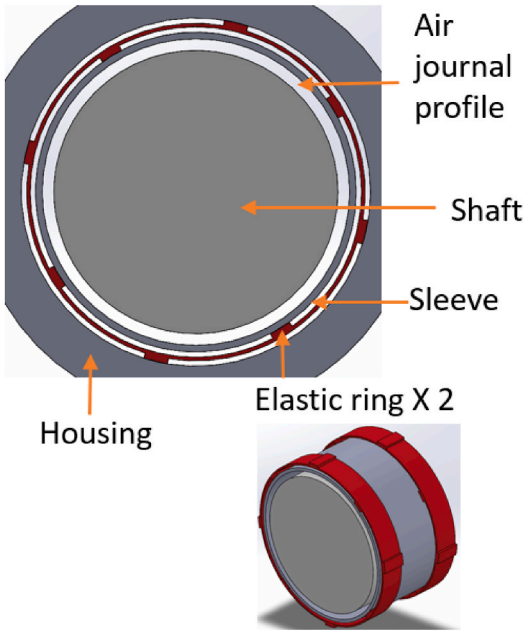

Fig. 1. Air journal bearing with elastic rings.

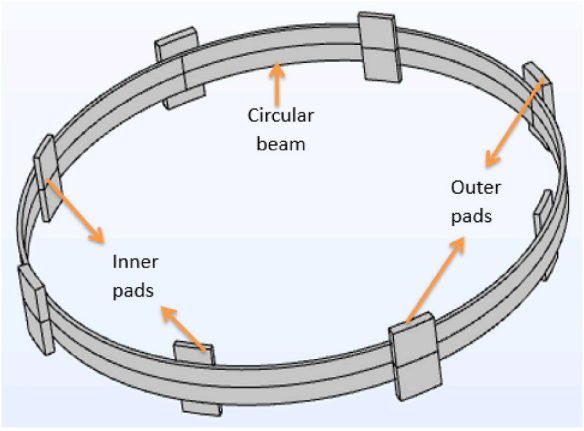

Fig. 2. Elastic ring layout.

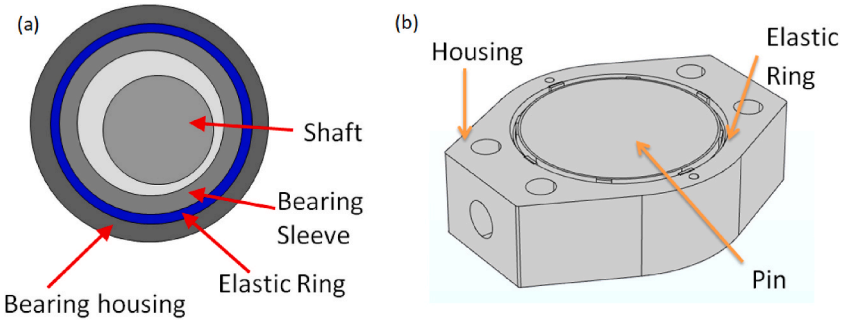

Fig. 3. Elastic ring position in (a) air journal bearing (b) simulations.

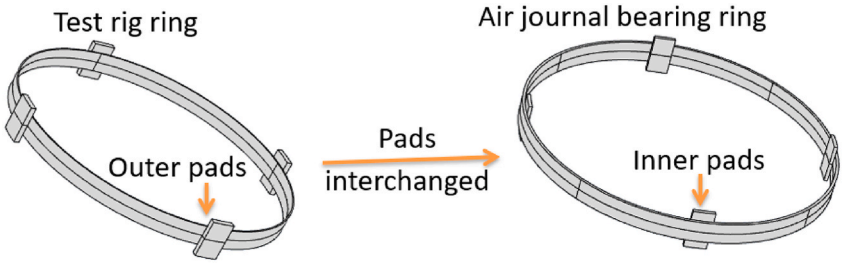

Fig. 4. Interchanging outer and inner pads.

become outer pads.

2.2. Simulation model physics

The following methods are generally used in literature [8]) to compute the response of elastic rings to different types of loads:

1. Euler or Timoshenko theories for vibrating beams [9].
2. Linear elastic material model [10].
3. Love's theory for general vibration of circular rings [11].
4. Theory of plate and shell [12].

After studying the recommended theories, it is concluded that solving the linear elastic material model with FEM to calculate the ring response is a suitable approach for the ring geometry, material, and boundary conditions. Using the linear elastic model was a good candidate since this model physics has a wide variety of boundary conditions to model the housing and pin interface. Also, the

elastic ring geometry has a non-uniform and irregular geometry since it has pads on its outer and inner surfaces as shown in Fig. 2.

The shell theory could have been a good candidate if the ring is always thin. Since different thicknesses and heights are theoretically analyzed for the rings, the shell theory couldn't be used. Also, Timoshenko theory for vibrating beams and Love's theory for general vibration of circular rings didn't take into consideration the pads extrusions in the elastic ring geometry.

2.3. Boundary conditions

The boundary conditions used in the simulations are cylindrical joints between the pin and the elastic ring, the elastic ring and the housing and a harmonic uniaxial boundary load on the housing as shown in Fig. 5. The cylindrical joint constraints the ring motion to a rotation about the pin longitudinal axis, or translation along the pin longitudinal axis. It also introduces a friction factor between the joint boundaries to model the friction between the pin and ring materials or the ring and housing materials.

A tetrahedral mesh was automatically generated by a commercial FEM program as shown in Fig. 6.

After obtaining the elastic rings dynamic response, the following formulas are used to obtain the stiffness and damping coefficients of the elastic rings [8]).

2.4. Elastic rings dynamic response

The response is calculated for the initial ring geometry in Fig. 2. The elastic ring response is obtained for harmonic forces having amplitudes ranging from 0 to 120 N and frequencies ranging from 300 to 2300 Hz. An automatic mesh is generated for the FEM model and a frequency domain solver is used. The dynamic response of the ring and the housing is shown in Fig. 7 (a), Figs. 7 (b) and Fig. 8 for an input force of 600 Hz frequency and 5 N amplitude. The ring deformation is calculated by subtracting the rigid housing displacement from the elastic displacement of the ring.

The stresses on the elastic ring are also calculated for all the combinations of the input force magnitudes and frequencies. It is found that stresses are smaller than the endurance strength of the elastic ring material. The stresses on the ring at an input force of 120 N amplitude and 2300 Hz frequency are shown in Fig. 9 (a).

Since there are no boundary conditions defined for the circular beam section of the elastic rings, the beam section is considered a free linear elastic body. An additional simulation requirement for the simulation model to be valid is to ensure that elastic ring deformation is smaller than the maximum clearance allowed between the circular beam section of the elastic ring and the housing (which is equal to outer pads thickness), and also smaller than the maximum clearance between the circular beam section and the pin (which is equal to inner pads thickness), If the clearance is not positive, then the elastic ring and the housing or the pin will overlap and the simulation won't be valid. The clearance is computed as the difference between the outer pad thickness and the radial ring deformation if the radial ring deformation is positive and the difference between radial ring deformation and the inner pad thickness if the ring radial deformation is negative. The clearance is calculated for all the cases and is found to be always positive.

Fig. 9 (b) shows the clearance at a force of 120 N amplitude and 2300 Hz frequency. Since all the simulation limitations are met, the simulation results can be used to estimate the stiffness and damping coefficients of the elastic ring.

2.5. Elastic ring dynamic coefficients

To find an appropriate model to obtain the dynamic coefficients of the rings using the ring dynamic response (see section 2.4), a review is done on the different methods used by other researchers to obtain the dynamic coefficients of elastic rings [13]. calculated the dynamic coefficients of elastic rubber rings using Kelvin Voigt model. The model computes the transfer function of the system in Laplace domain then computes the stiffness and damping coefficients [12]. calculated theoretically and verified experimentally the elastic ring stiffness. They considered the ring as an axisymmetric element and applied a fixed radial load at different angles between the two adjacent inner pads of elastic ring then measured the radial deformation. They calculated the stiffness as the ratio between the

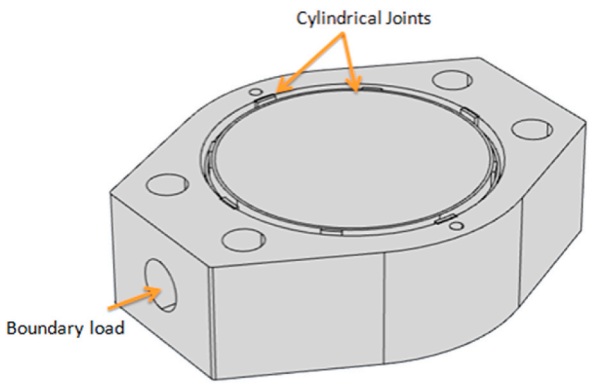

Fig. 5. Model boundary conditions.

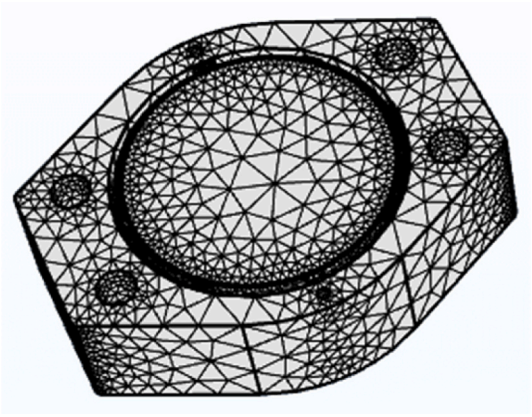

Fig. 6. Model tetrahedral mesh.

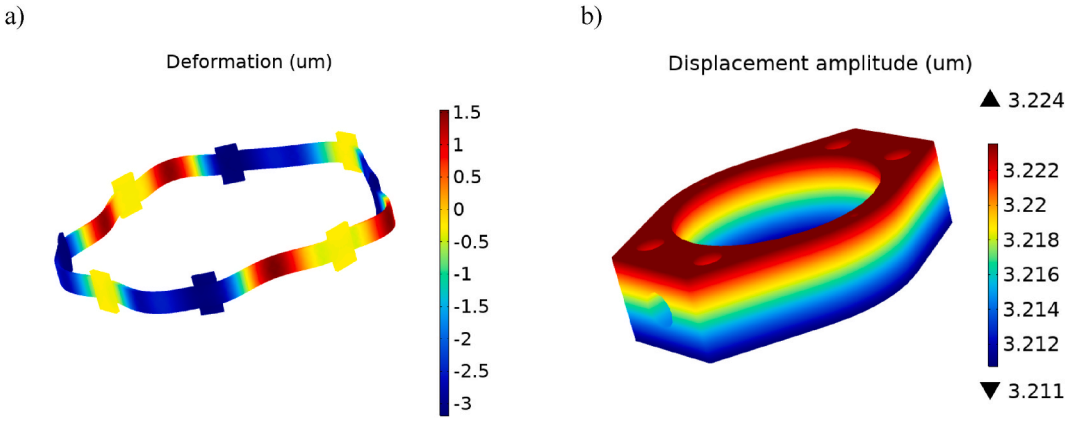

Fig. 7. (a) Ring deformation and (b) Housing response at 5 N and 600 Hz.

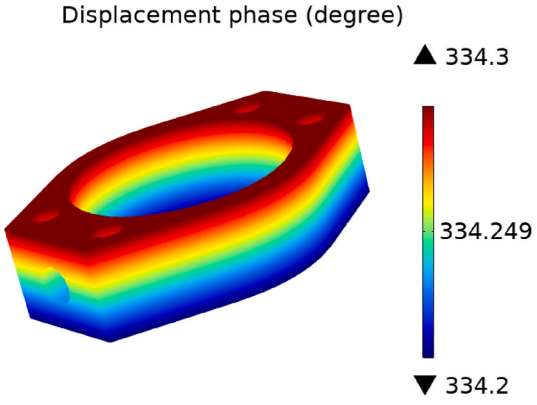

Fig. 8. Phase angle of the displacement for the Housing at 5 N and 600 Hz.

force and the maximum radial deformation. To obtain the dynamic coefficients of the elastic rings, a lumped mechanical model is constructed based on the constraints and the boundary conditions of the elastic ring. The elastic ring is enclosed between a moving housing and a fixed pin. The housing is excited by a uniaxial harmonic force. The mass of the ring is neglected compared to the mass of the housing. The housing-ring-pin system is equivalent to the lumped mass-spring-damper model shown in Fig. 10.

Fig. 11 shows the free body diagram describing the lumped model in Fig. 10 (see Fig. 12).

The equation of motion describing the model is

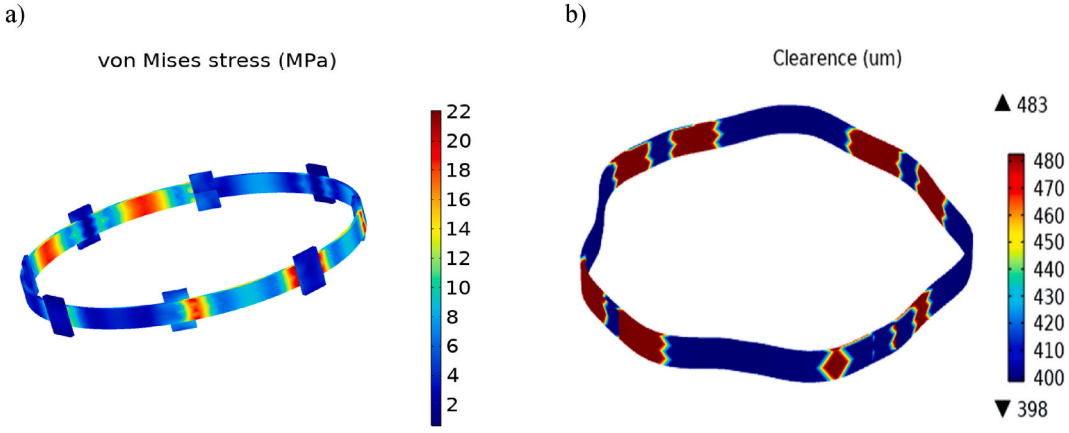

Fig. 9. (a) The stresses on the ring and (b) The clearance of the ring after being deformed at 120 N and 2300 Hz.

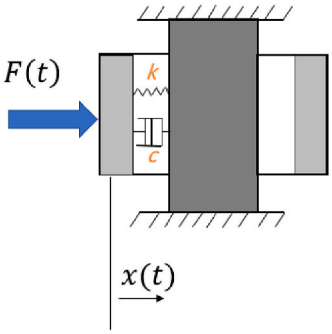

Fig. 10. Lumped mechanical model.

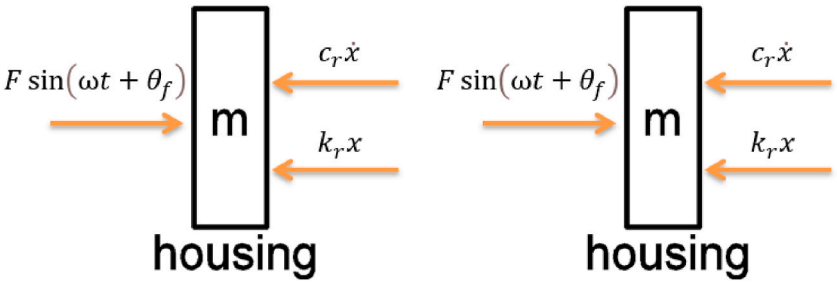

Fig. 11. Free body diagram of the lumped model.

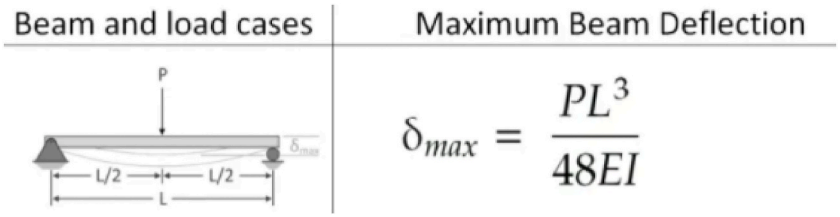

Fig. 12. Simply supported beam maximum deflection formula [14].

$$m\ddot{x} = F\sin(\omega t + \theta_f) - C_r\dot{x} - K_r x \tag{1}$$

where.

m is mass

$\ddot{x}$ is the acceletation of the system

C_r is the damping coefficient of the elastic ring

$\dot{x}$ is the velocity of the system

K_r is the stiffness coefficient of the elastic ring

x is the displacement of the system

F is the external force magnitude

ω is the angular frequency

t is time

θ_F is the phase angle of the external force

Eq. (1) is a second order non-homogeneous ordinary differential equation. The steady-state (particular) solution for this type of equation has the following form

$$x = X\sin(\omega t + \theta) \tag{2}$$

where.

X is the displacement magnitude of the system response

θ is the phase angle of the displacement of the response

Solving Eqs. (1) and (2) yields to:

$$C_r = \frac{F\sin(\theta_f - \theta)}{X\,\omega} \tag{3}$$

$$K_r = \frac{F\cos(\theta_f - \theta)}{X} + m\,\omega^2 \tag{4}$$

Where C_r *and* K_r are the elastic ring stiffness and damping coefficients respectively.

3. The effect of the elastic rings geometrical parameters on the dynamic coefficients

A review is done on the effect of the input force, input frequency, and elastic ring geometry on the stiffness and damping coefficients of the elastic rings [15]. calculated experimentally the stiffness and damping coefficients of elastomeric O-ring bearing mounts. Their results discuss the effect of changing different parameter on the coefficients of the rings. They concluded that increasing the frequency of the input force increases the stiffness coefficient of the elastic ring and increasing the amplitude of the input force decreases the stiffness and damping coefficients. The results are summarized as follow.

Factor	Stiffness Coefficient	Damping Coefficient
Vibrating Frequency	Increases	*No Steady Pattern
Temperature	Decreases	Decreases
Preload	Increases	Decreases
Ring Thickness	*No Steady Pattern	*No Steady Pattern
Vibration Amplitude	Decreases	Decreases

* No Steady Pattern: As the parameter changes, the dynamic coefficients change without pattern.

[13] concluded that the stiffness coefficient of the rings increases with frequency and the damping coefficient decreases with frequency. They also concluded that both stiffness and damping coefficients increase when the ring thickness increases. [78] calculated using FEM and verified experimentally the dynamic coefficients of squeezed O-rings used to support high-speed bearings of high-speed turbo machinery. The concluded that the stiffness coefficient of the O-rings increases with frequency [12]. studied theoretically and verified experimentally the influence of changing the number of the pads and the ring thicknesses on the ring stiffness. They concluded that the elastic ring stiffness increases with an increase in the number of the pads or the ring thickness.

3.1. Prediction model

Simply supported beam model is used to estimate the effect of the elastic ring geometry and material on the stiffness coefficient. In the model, the inner pads correspond to the simple support boundary, the outer pads represent the surface on which the boundary load is applied, and the ring beam sections correspond to the beam part of the model. The stiffness of a simply supported beam is directly proportional to the beam elastic modulus, section modulus and inversely proportional to the cubic power of the beam length.

3.2. Rings thickness

The effect of the ring thickness on the stiffness and damping coefficients is studied theoretically. Fig. 13 demonstrates a

visualization of the ring thickness variation.

After obtaining the forced dynamic response of the rings from FEM results, Eqs. (3) and (4) are used to obtain the theoretical stiffness and damping coefficients as shown in Fig. 14 and Fig. 15. It is clear from the figures that increasing the ring thickness slightly increases the stiffness and damping coefficients. The increase in damping coefficients is only effective as low frequencies. The increase in stiffness coefficients is only effective at high frequencies. Based on simply supported beam model (see section 3.1), an increase in the stiffness is expected since the stiffness of the simply supported beam is directly proportional with the section modulus of the ring which in turn increases when the thickness of the ring increase. The model prediction hence is in good agreement with the theoretical results obtained.

3.3. Rings height

The effect of the ring height on the stiffness and damping coefficients is studied theoretically. Fig. 16 demonstrates a visualization of the height variation.

The theoretical results shown in Fig. 17 and Fig. 18 have the same pattern as the results of changing the ring thickness (see section 3.2). Important thing to note is that increasing the height increases the stiffness and damping coefficients to higher magnitudes than increasing the ring thickness. Based on simply supported beam model, an increase in the stiffness is expected since the stiffness of the simply supported beam is directly proportional with the section modulus of the ring which in turn increases when the height of the ring increase.

3.4. Number of pads

The effect of the number of the pads on the stiffness and damping coefficients is studied theoretically. Fig. 19 demonstrates a visualization of the number of pads variation.

The theoretical results shown in Fig. 20 and Fig. 21 have the same pattern as the results of changing the ring height (see section 3.3). Important thing to note is that increasing the number of inner and outer pads increases the stiffness and damping coefficients to higher magnitudes than increasing the ring height. Based on simply supported beam model, an increase in the stiffness is expected since the stiffness of the simply supported beam is inversely proportional with the cube of the length of the beam and directly proportional with the ring cross section modulus which is the case for increasing the number of inner and outer pads since the beam length decreases when the number of inner pads increase and the section modulus increases when the number of outer pads increase (see Fig. 22).

To deduce whether the inner or outer pads effect has noticeable effect of the dynamic coefficients, the inner pads number and outer pads number is studied separately. The effect of the number of the inner pads on the stiffness and damping coefficients is studied theoretically. Fig. 19 demonstrates a visualization of the number of pads variation.

The effect of the number of the outer pads on the stiffness and damping coefficients is studied theoretically. Fig. 25 demonstrates a visualization of the number of pads variation.

The theoretical results shown in Fig. 23, Fig. 24, Fig. 26, and Fig. 27 shows that increasing the number of outer pads increases the stiffness and damping coefficients to higher magnitudes than increasing the number of inner pads.

3.5. Pads sector angle

The effect of the sector angle of the pads on the stiffness and damping coefficients is studied theoretically. Fig. 28 demonstrates a visualization of the pads sector angle variation.

The theoretical results shown in Fig. 29 and Fig. 30 have the same pattern as increasing the number of pads (see section 3.4). Important thing to note is that increasing the sector angle of the inner and outer pads increases the stiffness and damping coefficients to lower magnitudes than increasing the ring pads number (see section 3.4). Based on simply supported beam model, an increase in the stiffness is expected since the stiffness of the simply supported beam is inversely proportional with the cube of the length of the beam

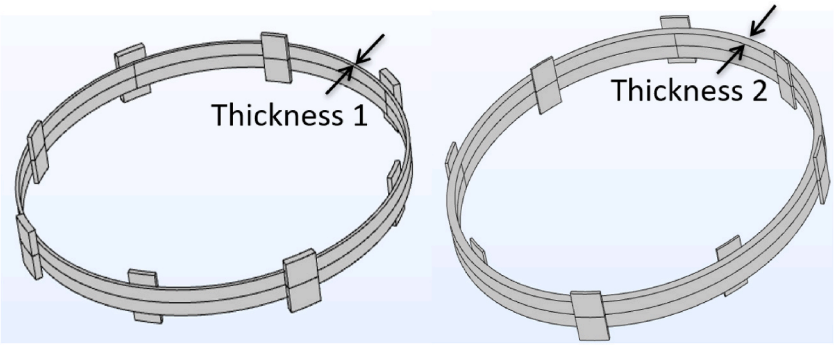

Fig. 13. Variation of ring thickness.

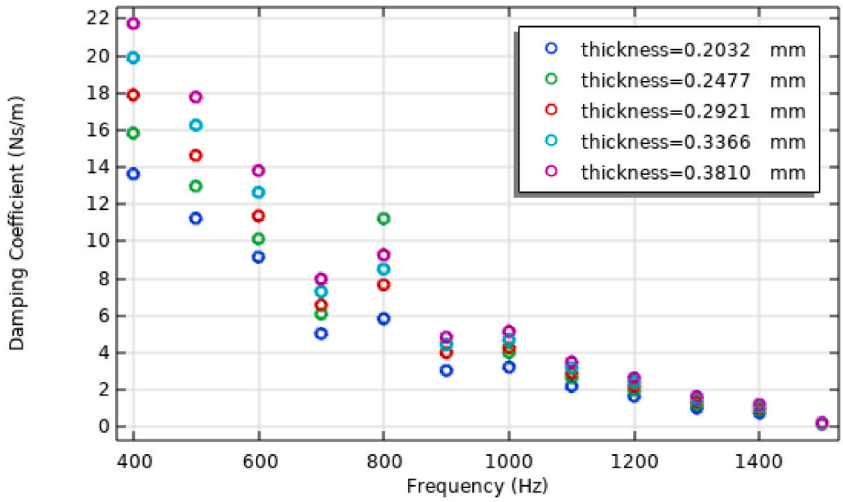

Fig. 14. Damping coefficient at different ring thickness.

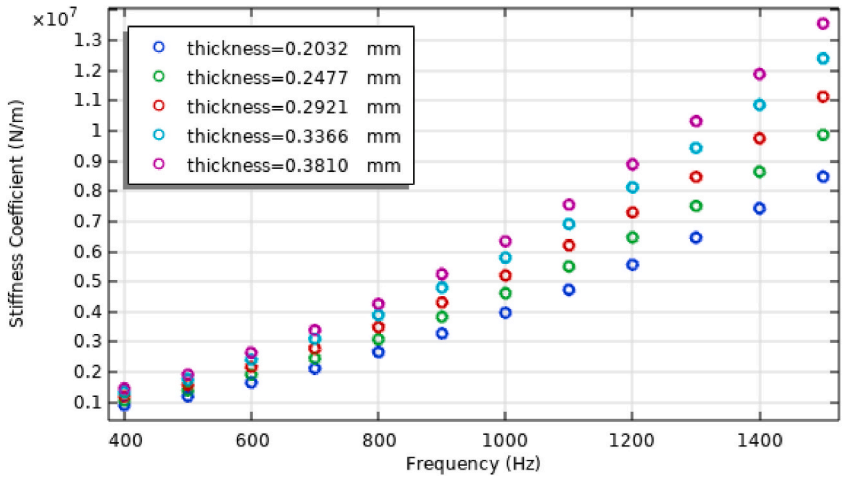

Fig. 15. Stiffness coefficient at different ring thickness.

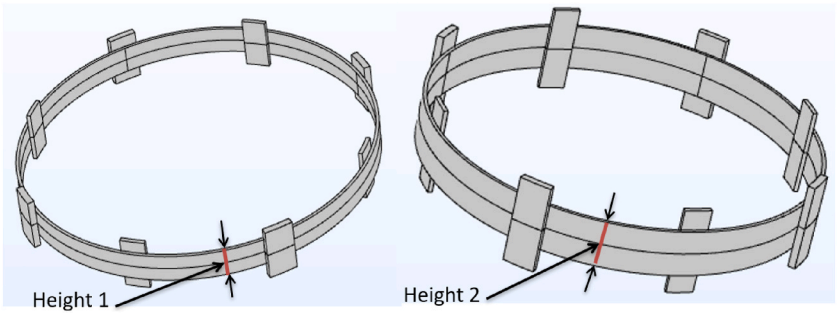

Fig. 16. Variation of the ring height.

and directly proportional with the ring cross section modulus which is the case for increasing the number of inner and outer pads sector angle since the beam length decreases when the inner pads sector angle increase and the section modulus increases when the outer pads sector angle increase.

To deduce whether the inner or outer pads sector angles have a noticeable effect of the dynamic coefficients, the inner pads number and outer pads number is studied separately. The effect of the sector angle of the inner pads on the stiffness and damping coefficients is

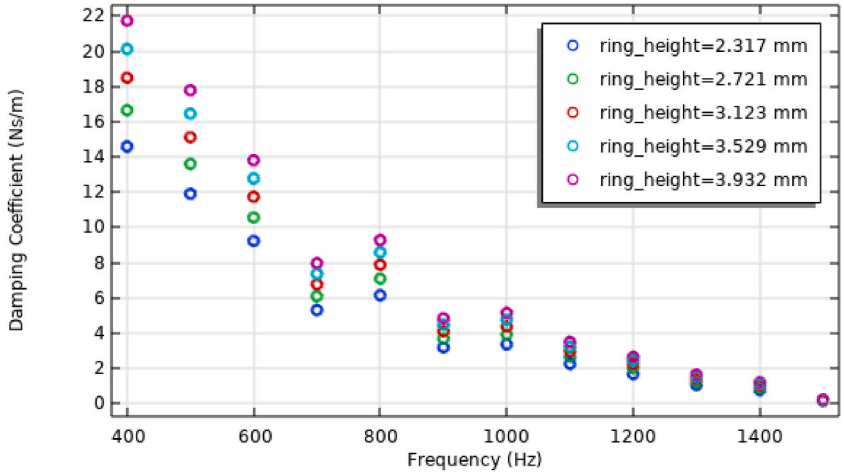

Fig. 17. Damping coefficient at different ring height.

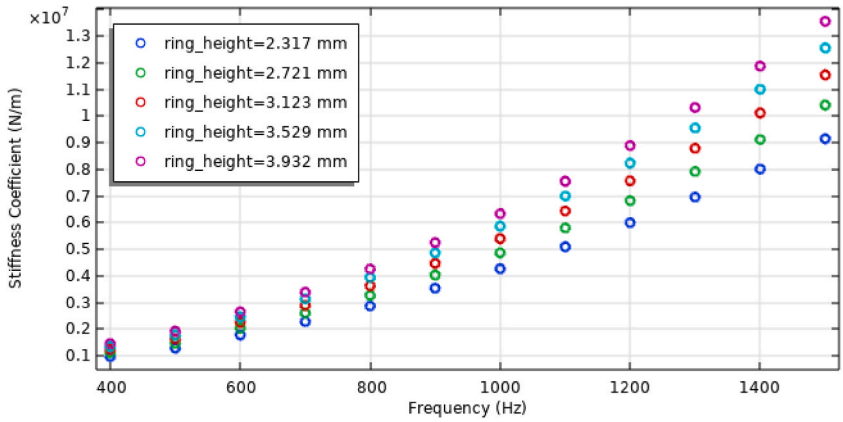

Fig. 18. Stiffness coefficient at different ring height.

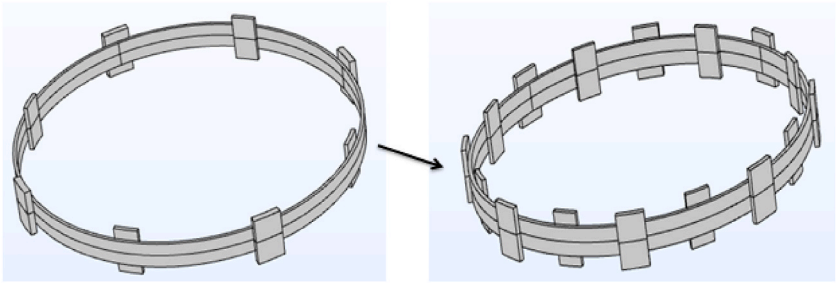

Fig. 19. Variation of the number of inner and outer pads.

studied theoretically. Fig. 31 demonstrates a visualization of the pads sector angle variation.

The effect of the sector angle of the outer pads on the stiffness and damping coefficients is studied theoretically. Fig. 34 demonstrates a visualization of the pads sector angle variation.

The theoretical results shown in Fig. 32, Fig. 33, Fig. 35, and Fig. 36, shows that increasing the number of inner pads sector angle increases the stiffness and damping coefficients to higher magnitudes than increasing the outer pads sector angle. After studying the geometrical parameters, it is concluded that increasing the number of the outer pads has the most effect on both stiffness and damping coefficients when compared to the other geometrical parameters.

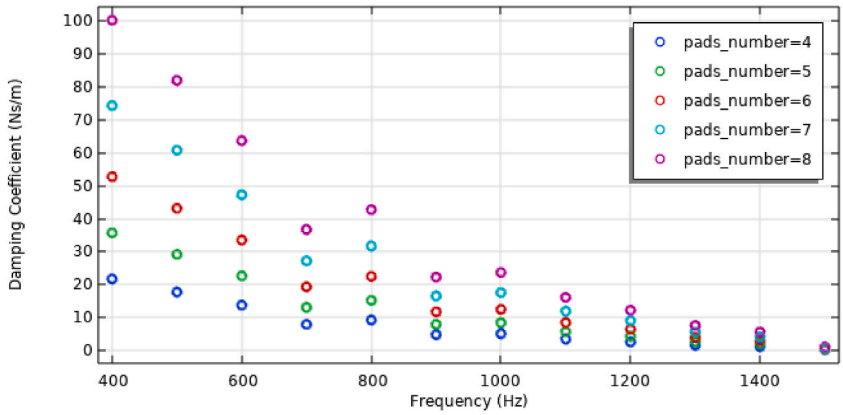

Fig. 20. Damping coefficient at different pads number.

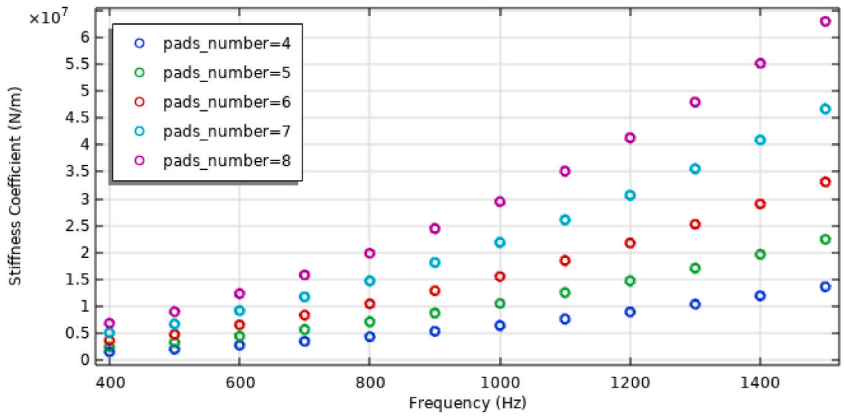

Fig. 21. Stiffness coefficient at different pads number.

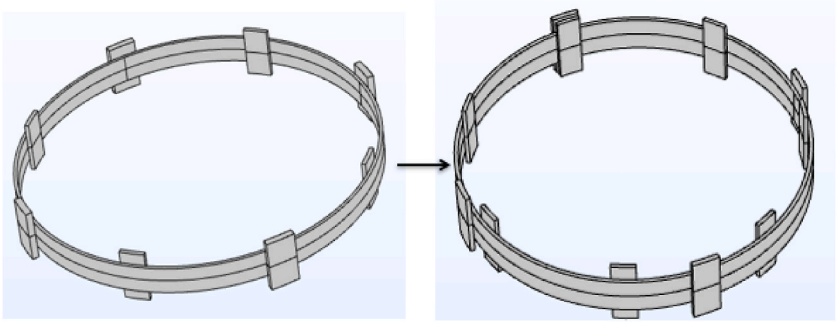

Fig. 22. Variation of the number of inner pads.

4. Neural network implementation

The discussed FEM results in section 2 covers the discrete geometrical cases where a single geometrical parameter is changed while the remaining parameters are fixed. Predicting the dynamic coefficients for all possible geometries using FEM would be computationally expensive [8]). To reduce the FEM computational power, a NN is trained using the discrete cases covered in section 2 to predict the dynamic coefficients for all possible ring geometries for the given ring geometrical parameters input domain which are:

- rings thickness of 0.2032–0.381 mm with 3 discrete values in between
- rings height of 2.317–3.932 mm with 3 discrete values in between

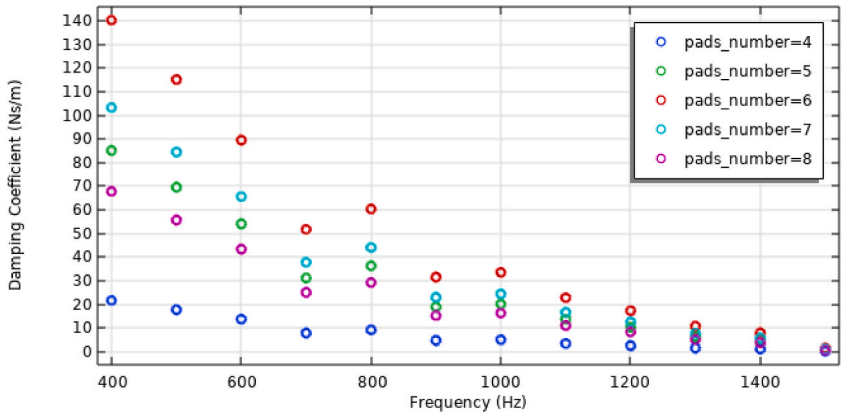

Fig. 23. Damping coefficient at different inner pads number.

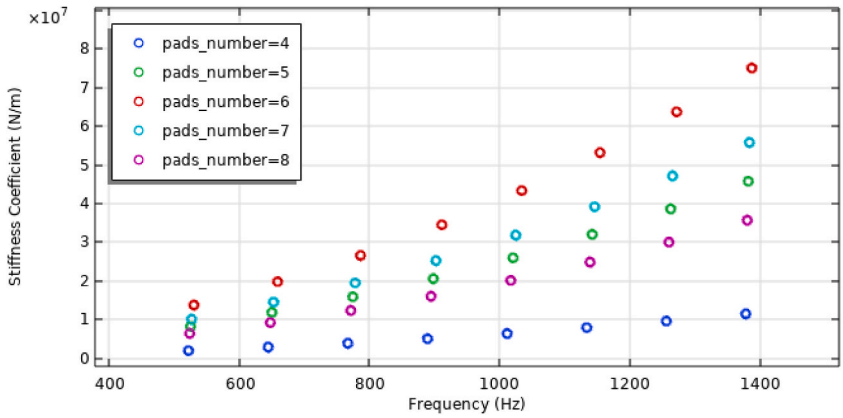

Fig. 24. Stiffness coefficient at different inner pads number.

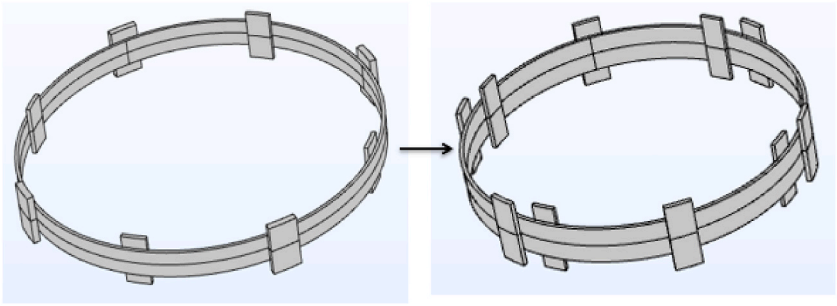

Fig. 25. Variation of the number of outer pads.

- inner pads number of 4–8 pads with a step of 1
- outer pads number of 4–8 pads with a step of 1
- inner pads sector angle of 8–45° with 8 discrete values in between
- outer pads sector angle of 8–45° with 8 discrete values in between

A feed forward neural network (NN) is then trained to obtain non-linear regression function that models the physical system for the given domains of the input parameters [16]. The NN inputs are the geometrical parameters of the rings and the harmonic force input frequency. The NN network output is the ring stiffness and damping coefficient. [65]. The accuracy of the trained NN to model the physical system is measured by computing the mean square error (MSE) of the NN (C [17].

To verify the trained NN model, NN results are plotted against FEM results in Fig. 37 and Fig. 38 for the initial rings geometry

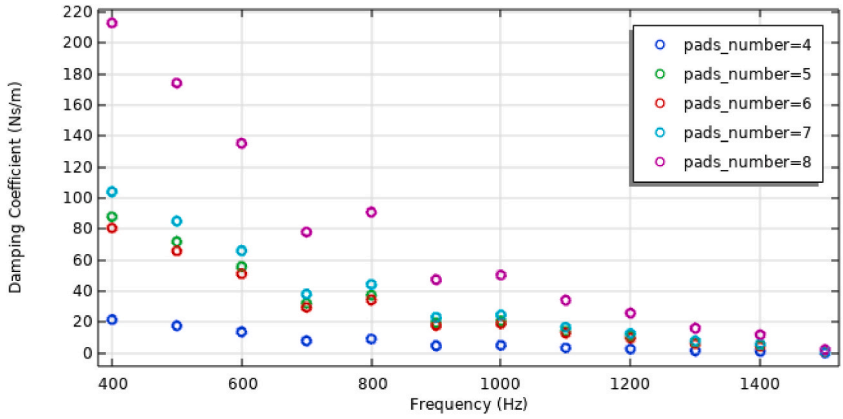

Fig. 26. Damping coefficient at different outer pads number.

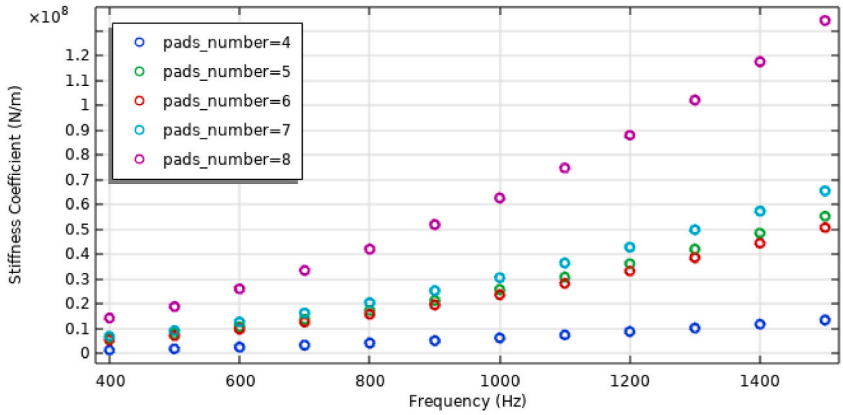

Fig. 27. Stiffness coefficient at different outer pads number.

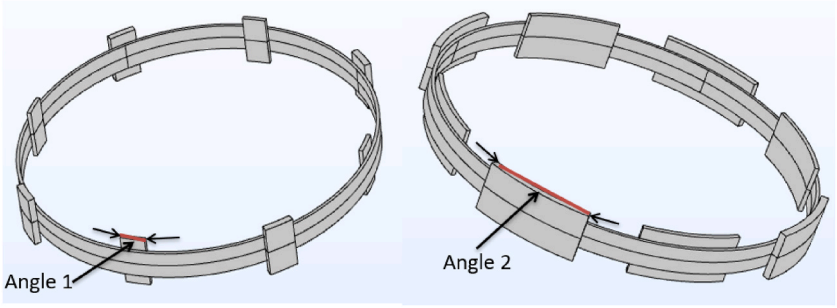

Fig. 28. Variation of the sector angle of the inner and outer pads.

demonstrated by Ref. [8]). The mean square error is less than 3%. Hence, the trained NN is able to predict the physics of the FEM model.

5. Conclusion

In this paper, the dynamic properties of the elastic rings used to support the sleeve of air journal bearings are theoretically analyzed. First, the geometry of the elastic ring and the constraints the air bearing imposes on the elastic rings are discussed.

A preliminary effort was performed to identify a suitable method to predict the response of the rings to different loads. By analyzing the geometry of the rings, the material properties and the boundary conditions it was concluded that the linear elastic material model can be used to calculate the response of the rings to different loads. The linear elastic material model was used to simulate the responses

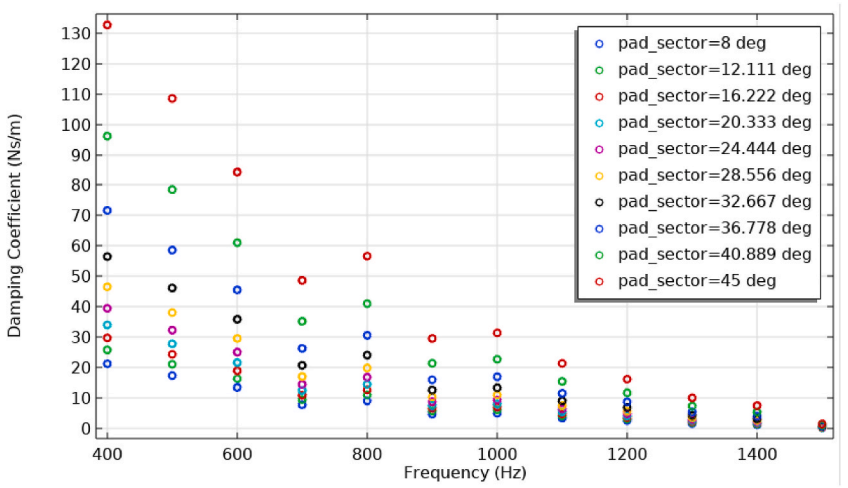

Fig. 29. Damping coefficient at different pads sectors.

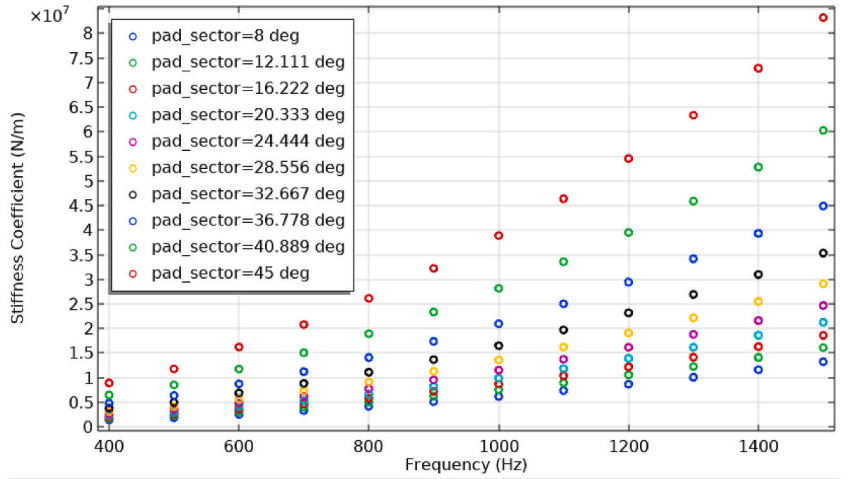

Fig. 30. Stiffness coefficient at different pads sectors.

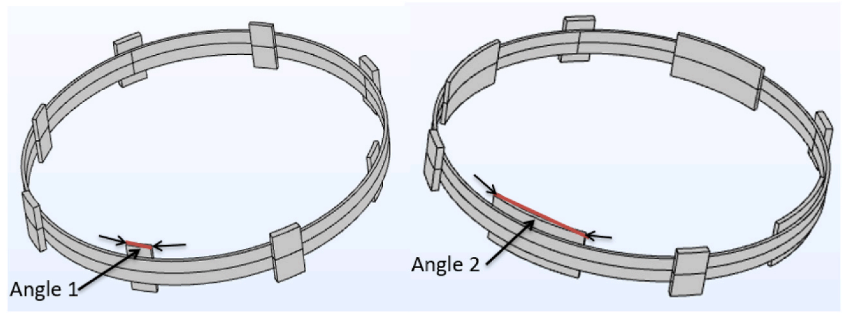

Fig. 31. Variation of the sector angle of the inner pads.

of the rings to harmonic forces with different frequencies and amplitudes. The responses were then used to calculate the stiffness and damping coefficients of the rings.

It was found that the stiffness coefficients increase with the input frequency, but the damping coefficients decrease very fast with the frequency. It was also found that the stiffness coefficient decreases, and the damping coefficient increases as the input force magnitude increases which agrees the results of [13,15].

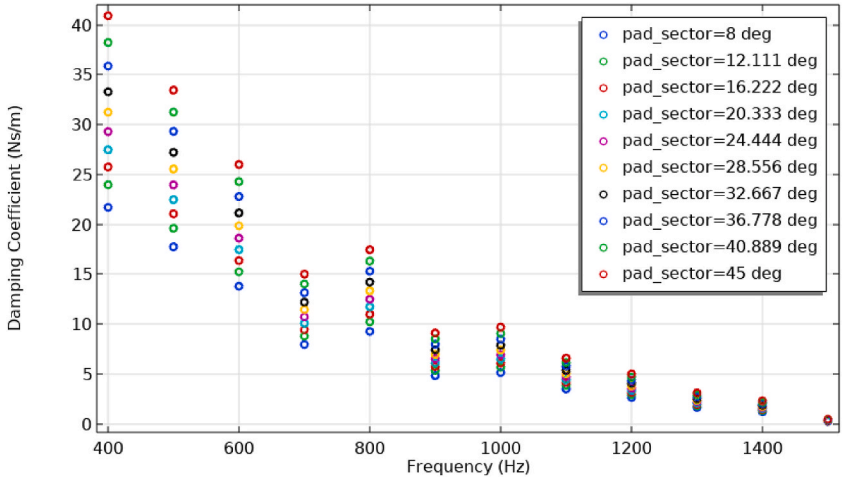

Fig. 32. Damping coefficient at different inner sectors.

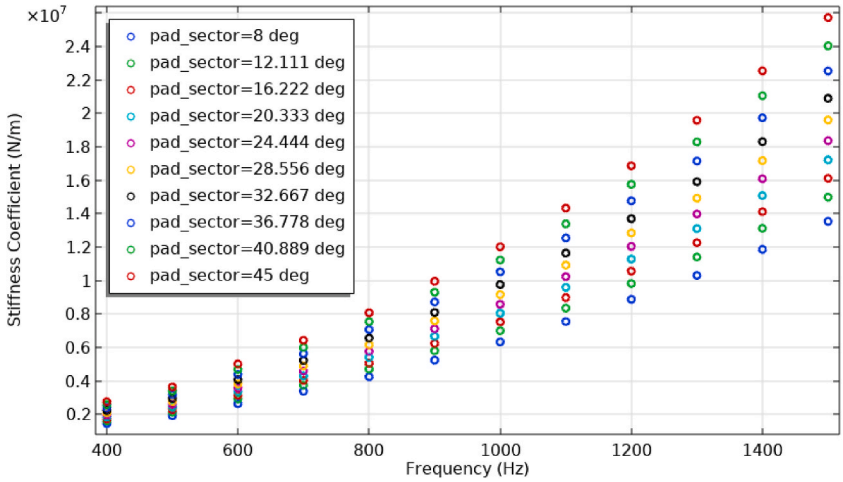

Fig. 33. Stiffness coefficient at different inner sectors.

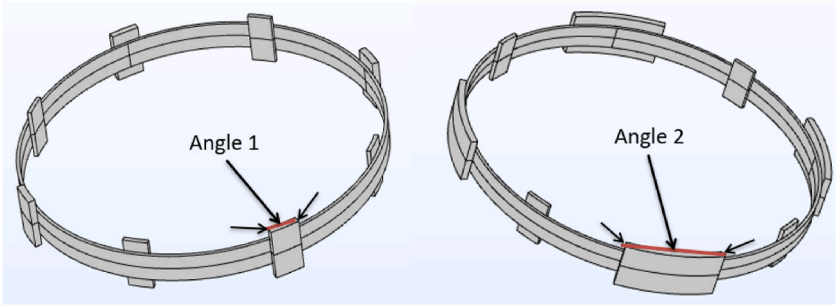

Fig. 34. Visualization of the sector angle of the outer pads.

The influence of the geometrical parameters of the rings on the stiffness and damping coefficients was next analyzed. A simplified model of the rings was also developed to predict the effect of the geometrical parameters on the stiffness coefficient. In this case, the ring is modeled as a group of simply supported beams connected to each other. Both the linear elastic material model and the simplified model predict that the stiffness coefficient increases when the thickness of the ring, the height of the ring or the elastic modulus of the ring material increases which agrees with the results of [12]. The stiffness and damping coefficients are then theoretically calculated

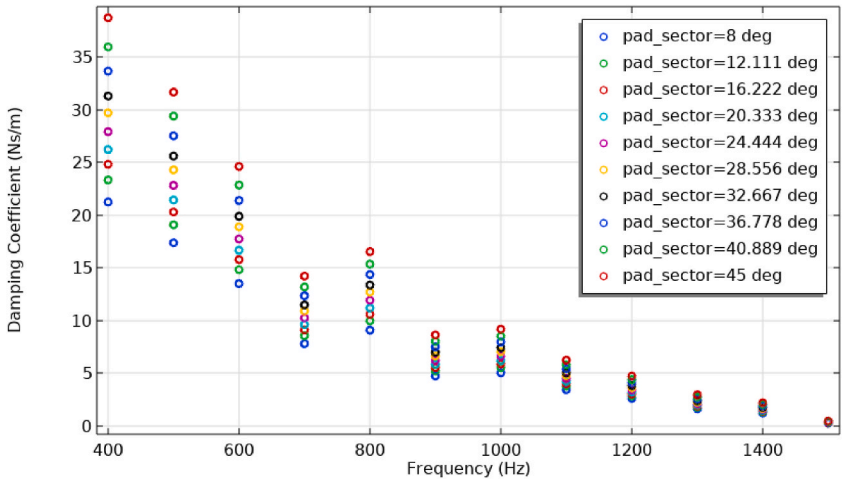

Fig. 35. Damping coefficient at different outer sectors.

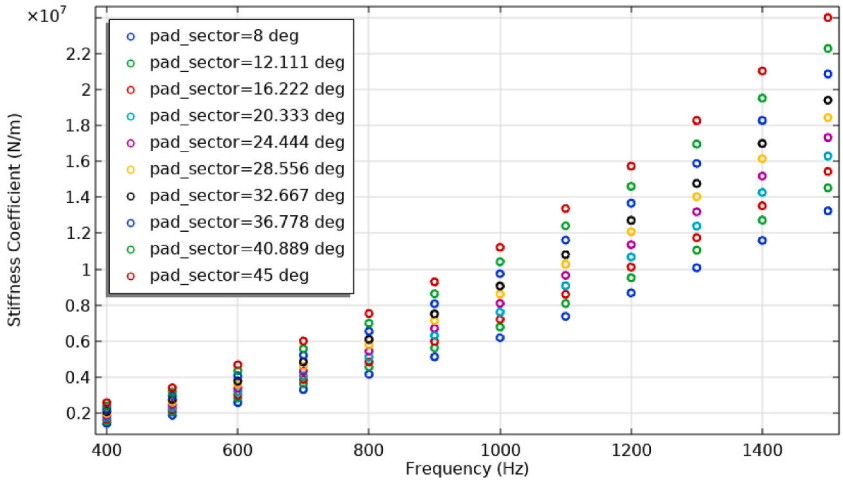

Fig. 36. Stiffness coefficient at different outer sectors.

for different ring geometries and different input force amplitudes and frequencies.

It is concluded that the stiffness coefficient increases, and the damping coefficient decreases as the input force frequency increases. Numerical simulations also shown that both the stiffness and damping coefficients increase slightly as the ring thickness increases or ring width increases. Both coefficients increase rapidly when the number of pads increases and the pads sector angle increases which agrees the experimental results of [12]. It is also noticed that increasing the number of the outer pads has the most effect on both stiffness and damping coefficients when compared to the other geometrical parameters.

A NN is then implemented predict the stiffness and damping coefficients of the elastic rings for any geometrical parameter combination of the elastic rings that fall within the given ring geometrical parameters input domain. The NN results are verified using validated FEM results of the rings dynamic coefficients [8]) and the results are in good agreement. The NN model hence can be used to describe the elastic rings physical model.

Author contribution statement

Ahmed Paridie: Conceived and designed the experiments; Performed the experiments; Analyzed and interpreted the data; Contributed reagents, materials, analysis tools or data; Wrote the paper.

Data availability statement

Data included in article/supp. material/referenced in article.

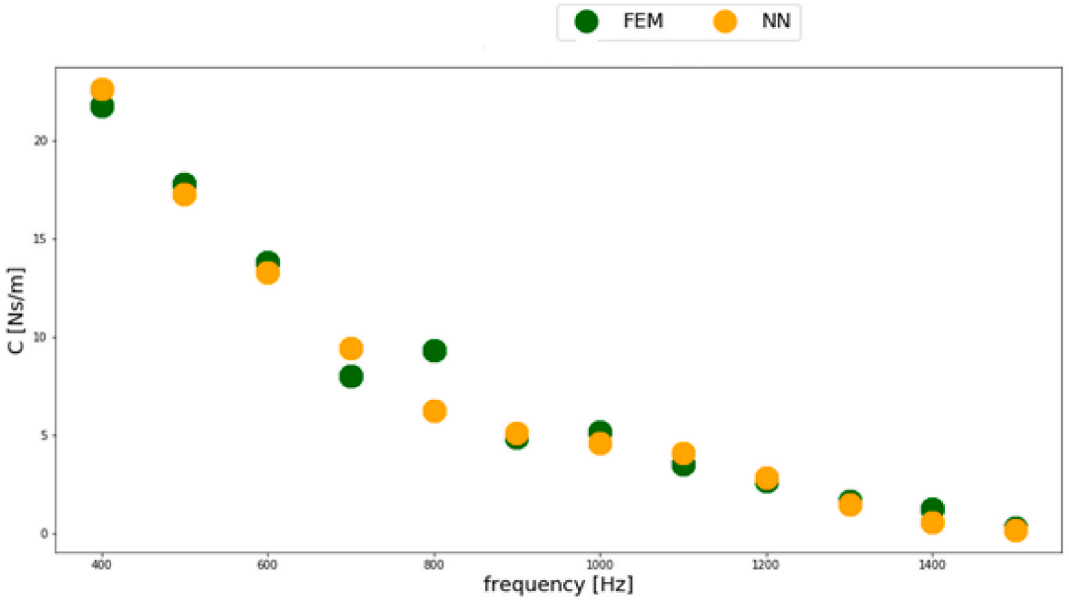

Fig. 37. Damping coefficient vs frequency for default rings ([22]).

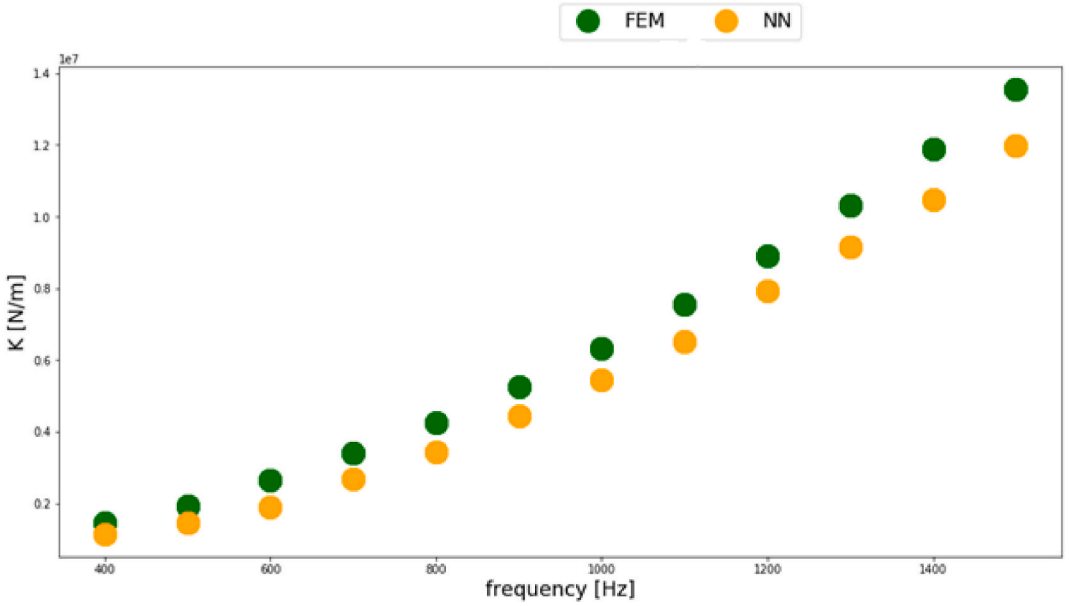

Fig. 38. Stiffness coefficient vs frequency for default rings ([22]).

Declaration of competing interest

The authors declare that this work was supported by the Office of Naval Research (Award No. N00014-19-1-2743).

References

[1] K. Czolczynski, Rotordynamics of Gas-Lubricated Journal Bearing Systems, springer, 1999.
[2] J.W. Lund, The stability of an elastic rotor in journal bearings with flexible, damped supports, J. Appl. Mech. (1965).
[3] B.C. Majumdar, Stability characteristics of gas-lubricated bearings supported on rubber "O" rings, Tribol. Int. (1975).
[4] S. Yoshimoto, Improvement of static characteristics of an aerostatic journal bearing using the elastic deformation of an O-ring, Tribol. Int. 20 (1987).
[5] Z. Wang, N. Xu, X. Yu, Z. Liu, G. Zhang, The Dynamic Characteristic Analysis of Elastic Ring Squeeze Film Damper by Fluid-Structure Interaction Approach, Proceedings of ASME Turbo Expo: Turbomachinery Technical Conference and Exposition, 2017.

[6] L. Zhao, M. Liao, J. Niu, Investigation on steady state unbalance response of rotor with elastic ring squeeze film damper, IOP Conf. Ser. Mater. Sci. Eng. 751 (2020), 012043.
[7] M. Jin, Y. Wang, J. Pan, Vibration of circular rings coupled by elastic elements, Appl. Acoust. 148 (2019) 264–275.
[8] Ahmed M. Paridie, Nicoleta M. Ene, Yasser S. Mohamed, Using neural networks to predict the effect of the preload location on the natural frequencies of a cantilever beam, Heliyon 8 (Issue 11) (2022), e11242, https://doi.org/10.1016/j.heliyon.2022.e11242. ISSN 2405-8440.
[9] D. Tounsi, J.B. Casimir, M. Haddar, Dynamic stiffness formulation for circular rings, Comput. Struct. 112–113 (2012) 258–265.
[10] T. Irvine, Ring Vibration Modes, 2015.
[11] T. Charnley, R. Perrin, V. Mohanan, H. Banu, Vibrations of thin rings of rectangular cross-section, J. Sound Vib. 134 (3) (1989) 455–488.
[12] Z. Han, Q. Ding, W. Zhang, Dynamical analysis of an elastic ring squeeze film damper-rotor system, Mech. Mach. Theor. 131 (2019) 406–419.
[13] F. Al-Bender, F. Colombo, D. Reynaerts, R. Villavicencio, T. Waumans, Dynamic characterization of rubber O-rings: squeeze and size effects, Advances in Tribology ume (2017), 2017, Article ID 2509879.
[14] R.C. Hibbler, Mechanics of Materials, eighth ed.", 2010.
[15] A.J. Smalley, M.S. Darlov, R.K. Mehta, Stiffness and Damping of Elastomeric O-Ring Bearing Mounts", National Aeronautics and Space Administration Lewis Research Center, 1977. Report No. CR-135328.
[16] A. Javadi, M. Moura, F. Asaad, A. Alireza, An artificial intelligence based finite element method, ISAST Transactions on Computers and Intelligent Systems 1 (2) (2009) 1–7. ISSN 1798-2448.
[17] C. German, SMART FINITE ELEMENTS: AN APPLICATION OF MACHINE LEARNING TO REDUCED-ORDER MODELING OF MULTI-SCALE PROBLEMS, Georgia Institute of Technology, 2019.
[22] K. Arnd, Deep Learning in the Finite Element Method, Institute of General Mechanics, RWTH Aachen University, Germany, 2021 thesis.
[65] Zheyue Mou, Bo Yan, Lin Xiang, Guizao Huang, Xin Lv, Prediction method for galloping features of transmission lines based on FEM and machine learning, Cold Reg. Sci. Technol. 173 (2020) 2020, https://doi.org/10.1016/j.coldregions.2020.103031, 103031, ISSN 0165-232X.
[70] J.W. Powell, M.C. Tempest, A Study of High-speed Machines with Rubber Stabilized Air Bearings, Journal of Lubrication Technology (1968).
[78] T. Shoyama, K. Fujimoto, Calculation of High-Frequency Dynamic Properties of Squeezed O-Ring for Bearing Support, Mechanical Engineering Journal 5 (2018).

Further reading

[18] S. Abrate, Vibration of non-uniform rods and beams, J. Sound Vib. 185 (4) (1995) 703–716.
[19] Samer Adeeb, Introduction to Solid Mechanics and Finite Element Analysis Using Mathematica, first ed.", 2012.
[20] F. Alefe, C. Saulo, P. Roque, S. Samir, A Machine Learning-Based Constitutive Model for Nonlinear Analysis via Finite Element Method, Dept. Of Structures Engineering, Federal University of Minas Gerais Av. Antonio Carlos, 6627, Pampulha, Belo Horizonte, 31270-901, 2020 (Minas Gerais, Brazil).
[21] M.H. Ang, W. Wei, L. Teck-Seng, On the estimation of the large deflection of a cantilever beam, in: Proceedings of the IECON'93 International Conference on Industrial Electronics, Control, and Instrumentation, vol. 3, 1993, pp. 1604–1609. Maui, HI, USA.
[23] V.M. Asnani, T.L. Krantz, D.C. Delap, The Vibration Ring", Glenn Research Center, 2014. NASA/TM—2014-218337.
[24] Maria Augusta Neto, et al., Engineering Computation of Structures: the Finite Element Method", E Book, first ed., Springer International Publishing, Switzerland, 2015.
[25] J.R. Banerjee, Dynamic stiffness formulation for structural elements: a general approach, Comput. Struct. 63 (1997).
[26] J.R. Banerjee, A. Ananthapuvirajah, S.O. Papkov, Dynamic stiffness matrix of a conical bar using the Rayleigh-Love theory with applications, European Journal of Mechanics and Solids 83 (2020), 104020.
[27] H. Bietz, V. Wittstock, Investigations to Determine the Dynamic Stiffness of Elastic Insulating Materials", 2018.
[28] R. Blevins, Formulas for Natural Frequency and Mode Shape", Krieger, Malabar, Florida, 1979.
[29] B. Bohn, J. Garcke, R. Iza-Teran, A. Paprotny, B. Peherstorfer, U. Schepsmeier, C.-A. Thole, Analysis of car crash simulation data with nonlinear machine learning methods, Proc. Comput. Sci. 00 (2013) (2013) 000–000.
[30] W. Chen, S. Chen, Z. Hu, J. Tang, H. Li, A novel dynamic model for the spiral bevel gear drive with elastic ring squeeze film dampers, Nonlinear Dynam. 98 (2019) 1081–1105.
[31] K. Czolczyíński, K. Marynowski, Stability of symmetrical rotor supported in flexibly mounted, self-acting gas journal bearings, Wear 194 (1996) 190–197.
[32] P. Cong, A.R. Magee, T. Zhang, Efficient calculation of the hydrodynamic coefficients and dynamic stiffness of an air-spring type vibration absorber, Ocean. Eng. 192 (2019), 106550.
[33] L. Cremer, M. Heckl, Damping behavior of cyclically deformed 304 stainless steel, Indian J. Eng. Mater. Sci. 10 (2003) 480–485.
[34] M. Darlow, E. Zorzi, Mechanical Design Handbook for Elastomers", 1981. Report 3423.
[35] Q. Ding, Dynamic Bearing Characteristics of Elastic Ring Squeeze Film Damper: Pressure Distribution, Ring Deformation and Contacts, Frontiers in Applied Mechanics, Ó Imperial College Press, 2016.
[36] NCEES FE Reference Handbook 10.0.1.
[37] A. Gasmi, P.F. Joseph, T.B. Rhyne, S.M. Cron, Closed-form solution of a shear deformable, extensional ring in contact between two rigid surfaces, Int. J. Solid Struct. 48 (2011) 843–853.
[38] Capuano German, Julian J. Rimoli, Smart finite elements: a novel machine learning application, 2019, Comput. Methods Appl. Mech. Eng. 345 (2019) 363–381, https://doi.org/10.1016/j.cma.2018.10.046. ISSN 0045-7825.
[39] G.M.L. Gladwell, N. Popplewell, The vibration of mechanical resonators (I): uniform rings and discs, J. Sound Vib. (1966) 343–350.
[40] G.M.L. Gladwell, The vibration of mechanical resonators (II): rings discs rods of arbitrary profile, J. Sound Vib. (1967) 351–364.
[41] T.H.E. Gulikers, Thesis, an Integrated Machine Learning and Finite Element Analysis Framework, Applied to Composite Substructures Including Damage, Faculty of Aerospace Engineering, Delft University of Technology, 2018.
[42] S. Ichisuzuki, Dynamic elastic response of a ring to transient pressure loading, J. Appl. Mech. (1966).
[43] D.J. Inman, Engineering Vibration, 2008.
[44] J. Kerr, The Onset and Cessation of Half Speed Whirl in Air Lubricated Self-Pressurized Journal Bearings, 1966. NEL Report No. 237.
[45] O. Kononenko, I. Kononenko, Machine Learning and Finite Element Method for Physical Systems Modeling, oleksiy.s.kononenko@gmail.Com.
[46] E. Kumar, R.K. Santosh, S.R. Teja, E. Abishek, Static and dynamic analysis of pressure vessels with various stiffeners, Mater. Today: Proc. 5 (2018) 5039–5048.
[47] Z.K. Laka, Dynamic Stiffness and Damping Prediction on Rubber Material Parts, FEA and Experimental Correlation", London Metropolitan University, 2016.
[48] T.E. Lang, Vibration of Thin Circular Rings Part I. Solutions for Modal Characteristics and Forced Excitation", 1962. Report No. 32-261.
[49] T.E. Lang, Vibration of Thin Circular Rings Part II. Modal Functions and Eigenvalues of Constrained Semicircular Rings", 1963. Report No. 32-261.
[50] Hyungmin Lee, Han-Seung Lee, Prannoy Suraneni, Evaluation of carbonation progress using AIJ model, FEM analysis, and machine learning algorithms, 2020, Construct. Build. Mater. 259 (2020), 119703, https://doi.org/10.1016/j.conbuildmat.2020.119703. ISSN 0950-0618.
[51] A.Y.T. Leung, W.E. Zhou, Dynamic stiffness analysis of axially loaded non-uniform timoshenko columns, Comput. Struct. 56 (4) (1994) 577–588.
[52] M. Li, J. Chen, R. Zhu, C. Duan, S. Wang, X. Lu, Dynamic Stiffness and Damping Characteristics of a Shaft Damping Ring: A Combined Hyper Elastic and Viscoelastic Constitutive Model", Hindawi Shock and Vibration, 2020. Article ID 8822760.
[53] L. Liang, M. Liu, C. Martin, W. Sun, A deep learning approach to estimate stress distribution: a fast and accurate surrogate of finite-element analysis, J. R. Soc. Interface 15 (2018), 20170844, https://doi.org/10.1098/rsif.2017.0844.
[54] W. Liu, Diss, Experimental and Analytical Estimation of Damping in Beams and Plates with Damping Treatments", University of Kansas School of Engineering, 2008.

[55] C.Q. Liu, G.M. Goetchius, Estimation of damping loss factors by using the hilbert transform and exponential average method, Journal of passenger car: mechanical systems journal (2001) 1496–1499. SAE Transactions, Vol. 110, Section 6.
[56] M. L Liu, C. Martin, W. Sun, A deep learning approach to estimate stress distribution: a fast and accurate surrogate of finite-element analysis, J. R. Soc. Interface 15 (2018), 20170844, https://doi.org/10.1098/rsif.2017.0844.
[57] L. Los Andres, S. Jeung, Response of a squeeze film damper-elastic structure system to multiple and consecutive impact loads, J. Eng. Gas Turbines Power 138 (2016).
[58] A. Love, A Treatise of the Mathematical Theory of Elasticity, fourth ed.", Cambridge University Press, London, England, 1927.
[59] Z. Lu, D. Gu, Ding Hu, W. Lacarbonara, L. Chen, Nonlinear Vibration Isolation via a Circular Ring", 2019, https://doi.org/10.1016/j.ymssp.2019.106490.
[60] Z. Lu, D. Gu, H. Ding, W. Lacarbonara, L. Chen, Nonlinear vibration isolation via a circular ring, Mech. Syst. Signal Process. 136 (2020), 106490.
[61] M.A. Mahmoud, Eigenvalues and dynamic stiffness of picket-shaped cantilevers, Sensor. Actuator. 304 (2020), 111872.
[62] R.E. Maringer, Damping Capacity of Materials, ume I", Battelle Memorial Institute Columbus Laboratories, 1966. Contract No. DA- 01- 021- AMC- 11706 (Z).
[63] R.D. Mindlin, L.E. Goodman, Beam vibrations with time-dependent boundary conditions, J. Appl. Mech. 17 (1950) 377–380, trans. ASME, vol. 72.
[64] R.K. Mittal, Flexure of a thin elastic ring due to a dynamic concentrated load, Int. J. Eng. Sci. 14 (1976) 241–257.
[66] M. Muthanandam, S. Thyageswaran, Determination of dynamic coefficients of air-ring bearings, Journal of Vibration Engineering & Technologies (2020).
[67] H. Ozturk, In-plane free vibration of a pre-stressed curved beam obtained from a large deflected cantilever beam, Finite Elem. Anal. Des. 47 (3) (2011) 229–236, https://doi.org/10.1016/j.finel.2010.10.003.
[68] S.O. Papkov, J.R. Banerjee, Dynamic stiffness formulation and free vibration analysis of specially orthotropic Mindlin plates with arbitrary boundary conditions, J. Sound Vib. 458 (2019) 522–543.
[69] A. Paridie, A study of the dynamic properties of the elastic rings of an air journal bearing [Master's thesis, University of Toledo]. OhioLINK Electronic Theses and Dissertations Center. http://rave.ohiolink.edu/etdc/view?acc_num=toledo1639401847150891, 2021.
[71] L.S. Prado, T.G. Ritto, Vibration reduction of a rotating machine using resonator rings, Mech. Res. Commun. (2020), 103533.
[72] Zhenchao Qi, Nanxi Zhang, Yong Liu, Wenliang Chen, Prediction of mechanical properties of carbon fiber based on cross-scale FEM and machine learning, Compos. Struct. 212 (2019), https://doi.org/10.1016/j.compstruct.2019.01.042, 2019, Pages 199-206, ISSN 0263-8223.
[73] M.F. Ranky, B.L. Clarkson, Frequency average loss factors of plates and shells, J. Sound Vib. 89 (3) (1983) 309–323.
[74] R.J. Schmidt, A.P. Boresi, Advanced Mechanics of Materials, sixth ed.", 2002.
[75] H. Schwieger, Report, vol. 17, Institut fiir Konstruktiven Ingenierbau", Ruhr University, Bochum, 1973, p. 25.
[76] L.J. Segerling, Applied Finite Element Analysis", 1984.
[77] W.M. Shepherd, F.A. Gaydon, Plastic Bending of a Ring Sector by End Couples, J. Mech. Phys. Solid. 5 (1957) 296–301 (Pergsmon Press Ltd., London).
[79] G.C. Silva, V.C. Beber, D.B. Pitz, Machine learning and finite element analysis: An integrated approach for fatigue lifetime prediction of adhesively bonded joints, Fatig. Fract. Eng. Mater. Struct. 44 (12) (2021) 3334–3348, https://doi.org/10.1111/ffe.13559.
[80] A. Sytin, A. Rodichev, A. Babin, Experimental Study of Foil Gas-Dynamic Bearing Elastic Elements Deformation, International Conference on Industrial Engineering, ICIE 2017, Procedia Engineering 206 (2017) 334–339.
[81] P.S. Varoto, L.P. R.d. Oliveira, On the force drop off phenomenon in shaker testing in experimental modal analysis, Shock Vib. 9 (2002) 165–175.
[82] P. Vurtur Badarinath, M. Chierichetti, F. Davoudi Kakhki, A Machine Learning Approach as a Surrogate for a Finite Element Analysis: Status of Research and Application to One Dimensional Systems, Sensors 21 (2021) 1654, https://doi.org/10.3390/s21051654, 2021.
[83] Y. Wang, Y.L. Yang, S. Wang, Z.L. Huang, T.X. Yu, Dynamic behavior of circular ring impinging on ideal elastic wall: Analytical model and experimental validation, by, International Journal of Impact Engineering 122 (2018) 148–160.
[84] Young Weaver Timoshenko, Vibration Problems in Engineering", Wiley Interscience, New York, 1990.
[85] H. Wei, Q.X. Pan, O.B. Adetoro, E. Avital, Y. Yuan, P.H. Wen, Dynamic large deformation analysis of a cantilever beam, Math. Comput. Simulat. 174 (2020) 183–204, https://doi.org/10.1016/j.matcom.2020.02.022. ISSN 0378-4754.
[86] J. Zhang, R.J. Perez, E.J. Lavernia, Documentation of damping capacity of metallic, ceramic and metal-matrix composite materials, J. Mater. Sci. 28 (1993) 2395–2404.
[87] C. Zhang, G. Jin, T. Ye, Y. Zhang, Harmonic response analysis of coupled plate structures using the dynamic stiffness method, Thin-Walled Struct. 127 (2018) 402–415.